

Performance Comparison of Wireless pH Sensor Modules for Application to Health Monitoring

Short Paper

Lan Zhang, Jian Lu, and Ryutaro Maeda

Device Technology Research Institute
National Institute of Advanced Industrial Science and Technology (AIST)
Tsukuba, Ibaraki 305-8564, Japan
e-mail: chou-ran@aist.go.jp
e-mail: jian-lu@aist.go.jp
e-mail: maeda-ryutaro@aist.go.jp

Abstract— The paper presents a compact pH sensor system and its extension to health monitoring, particularly for monitoring the urine of infants. Three types of sensing electrodes, namely, plate, comb, and pillar, are fabricated and evaluated to determine the suitable approach for different application requirements. Moreover, to realize a highly compact pH sensor system with a biofriendly interface that offers good user experience, a highly compact transmission module and new sensing materials are introduced to optimize the sensor structure and measurement system. Sensing electrodes fabricated with different materials are characterized comprehensively; two types of wireless transmission boards are proposed and compared. Temperature calibration is adaptably performed for the wider application of the proposed pH sensor system. The results indicate that the performance of the proposed compact pH system with a wireless transmission function is adequate and it can monitor the urine condition of infants in real time. In addition, the proposed pH sensor system can be used for healthcare, well-being, and medical applications.

Keywords-pH; field effect transistor; health condition; calibration; radio frequency; Bluetooth.

I. INTRODUCTION

Infant diseases, also known as childhood illnesses, can infect children several months after birth. Serious infant diseases include pertussis, *Candida albicans* infection, and measles, which may lead to death, if not detected in time [1] [2]. Parents are becoming increasingly concerned about their children's health. The detection and prevention of infant diseases is a critical task for doctors as well as researchers. Hence, the related products for infant health monitoring, which are in great demand worldwide, need to be developed as soon as possible [3].

The detection of physicochemical and biological parameters is generally based on three main types of media: blood, saliva, and urine [4]. A typical process for biological detection involves professional staff, such as nurses, who obtain samples from the target person, after which these samples are collected and sent to the designated laboratory for analysis. In general, such tests require several hours to days, according to the procedural difficulty. The real-time

monitoring of pathological parameters can efficiently indicate the health condition of infants and provide a reference to doctors for early treatment. However, blood specimen collection is an invasive sampling procedure, and after the sampling process, the target needs to hold a small gauze pad over the puncture site for a few minutes to stop the bleeding. Although saliva sampling is a noninvasive method, it is still challenging because the suitability of the collection method for the analyte of interest has not been sufficiently investigated. Among these physicochemical media, real-time monitoring of urine is the easiest approach. This is because a urine sensor can be placed in the diaper and can monitor the urine condition continuously without affecting the normal life of the infant [5][6].

Of late, there have been several developments in silicon-based microelectromechanical system (MEMS) technology, such as the realization of highly compact sizes and high performances [7][8][9][10]. Using the MEMS process, we have fabricated a highly compact pH sensor that has already been applied not only in chemical engineering but also in other fields such as agriculture and industry [11][12]. In this study, previous as well as latest work on the fabrication and evaluation of the improved pH sensor electrodes and wireless transmission approaches has been summarized. Moreover, extension of the application of the proposed sensor for health monitoring has been discussed. We modify the pH sensor system and casing method and optimize the sensing material of the electrode with a biofriendly surface such that it can be suitable for monitoring the urine of infants in the diaper. The settings of the sensors placed in the diapers of newborns are not well-developed for neonatal health monitoring. For monitoring neonatal conditions, nurses usually need to use traditional sensors (temperature or pH sensors) to measure the urine in the diapers every few hours. The efficiency of this method is very low, and precision is hard to guarantee. The sensor system developed in this paper, using MEMS technology and a wireless transmission method, can greatly improve work efficiency, save time, and enhance measurement precision.

Fig. 1 depicts the wireless pH sensor system and its potential applications as well as the proposed pH sensor electrodes. The sensor system mainly includes the sensing

electrodes and measurement and transmission PCBs (inset images). The electrodes are connected to the gate terminal of a metal-oxide-semiconductor field-effect transistor (MOSFET) on the measurement board for measuring the pH value of the target solution [11]. The electrodes were fabricated using the MEMS technique for realizing high-dimension and performance homogeneity. To determine the appropriate approach for health monitoring, we fabricated and evaluated three types of sensing electrodes, the plate, comb, and pillar type, to detect the urine in the diaper. Different sensing materials such as indium tin oxide (ITO), stannic oxide (SnO_2), tantalum pentoxide (Ta_2O_5), and antimony (Sb) were evaluated and compared. Two types of wireless transmission boards based on the radio frequency and Bluetooth techniques were proposed and evaluated (Fig. 1, left). Moreover, temperature calibration was adaptably performed for practical application of the proposed pH sensor system. Based on a smart phone Android operating system with an easy-to-use user interface, a barrier-free operating system was developed. The measured data can be obtained through a wireless transmission function. After stability testing through field measurements, several potential applications can be considered (Fig. 1, right). The compact sensing system unit can be placed in a diaper for real-time monitoring of the health of children or elders. Moreover, the compact sensor can be packaged with a biofriendly surface. The ultrasmall low-power wireless sensor node can also be implanted into the body of a pet animal to measure its body fluid condition. The rest of the paper is organized as follows. Section II presents experimental setup and procedure; Section III presents measurement results and Section IV introduces the user interface of the proposed pH sensor based on an android smartphone. Finally, Section V summarizes the paper.

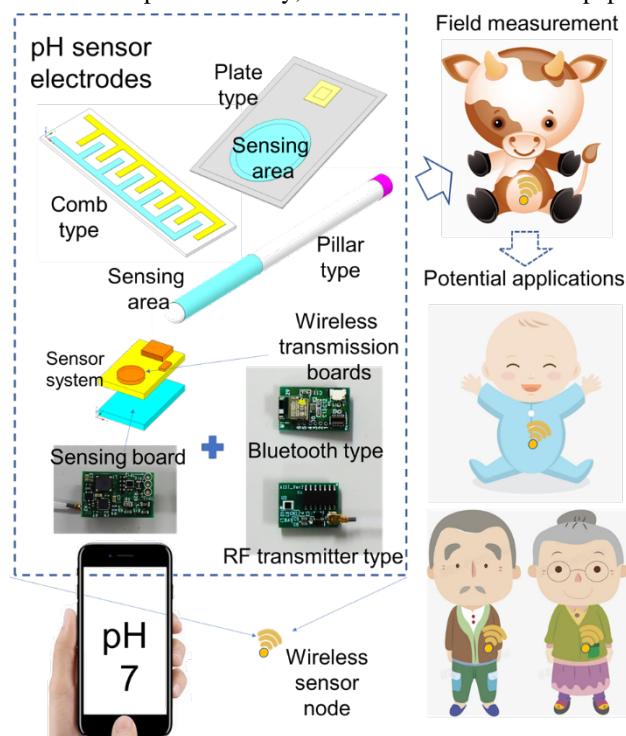


Figure 1. Wireless pH sensor system and its potential applications.

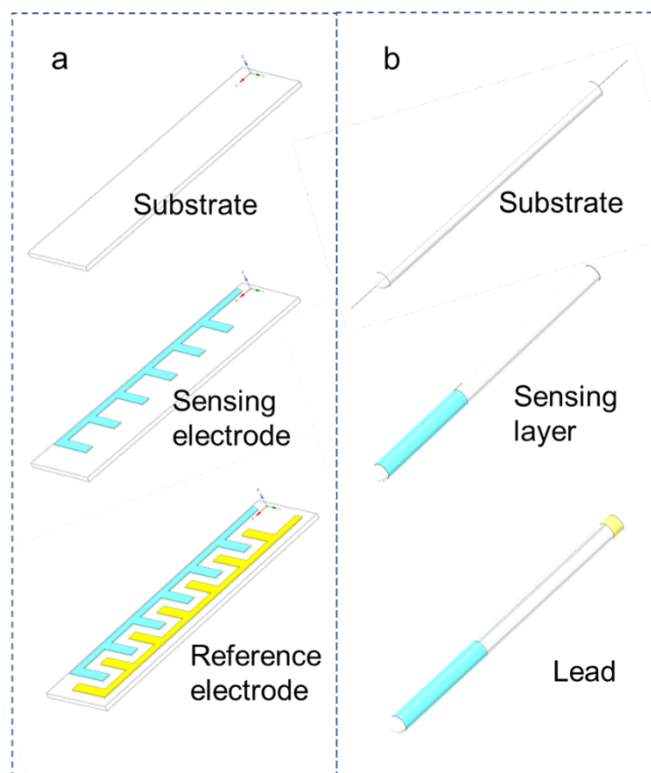


Figure 2. (a) Comb and (b) pillar pH electrode fabrication sequence.

II. EXPERIMENTAL SETUP AND PROCEDURE

A. Design and fabrication of the pH-sensing electrodes

We designed, fabricated, and evaluated plate, comb, and pillar type sensing electrodes. The fabrication process of a plate-type sensing electrode has been presented in our previous work [11]. Similar processes can be used to fabricate the comb and pillar structures. The comb electrode was fabricated through a micromachining process using three photomasks. Fig. 2a illustrates the comb electrode fabrication sequence. The device substrate was fabricated by polishing a glass wafer with a thickness and diameter of $200\ \mu\text{m}$ and $100\ \text{mm}$, respectively. A 100-nm sensing material layer was initially deposited on the surface of the glass substrate through a sputtering process. The sensing electrodes were then patterned through photolithography and an etching process. Finally, using the sputtering and liftoff processes, the reference electrode was generated and patterned (see Fig. 2a). Fig. 2b shows the fabrication sequence of the pillar-type electrode. By sputtering with uniform rotation, a 150-nm -thick sensing material layer was deposited on the cylindrical surface of a 5-mm diameter glass pillar. Then, using photolithography, sputtering, and liftoff, the lead and connecting electrodes were generated on the pillar electrode (see Fig. 2b). A highly compact reference electrode (R2K712, Toyorika Co.) was selected for the pH sensor system.

B. Fabrication of the measurement system

An 18 mm × 12 mm measurement board was fabricated, which included a sensing unit, the related power supply units, and a standard inter-integrated circuit (I²C) interface. In our previous work, the measurement board of the pH sensing system and the test philosophy have been described [11]. The n-type channel of the MOSFET is the sensing unit of the measurement system, which is connected to the sensing electrode for measuring the H⁺ density of the measured solution.

In the power supply units, DC/DC converters and regulators are used for the voltage drain and provide the reference voltage between the reference electrode and ground. I²C (INA 231, Texas Instruments Inc.) has 16-bit analog-to-digital converters for recording the measured analog data.

C. Design and fabrication of the wireless transmission system

Two types of control and transmission modules, a radio frequency integrated circuit (RFIC) and Bluetooth board, are introduced here. The specification and performance of the RFIC for animal testing are mentioned in our previous work [13]. An RFIC with a low-power type Si4010, which is a fully integrated crystal-less RF transmitter with an embedded microcontroller unit (CIP-51 8051), was selected. The transmission approach included a transmitter but not a transceiver because power consumption is crucial in health monitoring devices. The transmitter method can efficiently reduce the standby current by a factor of 100 [13], and the power consumption of the system can be reduced by several orders correspondingly.

Fig. 3 displays the front and back images of the Bluetooth transmission board as well as its circuit diagram. A four-layer PCB with a thickness of 1.6 mm was employed, and the fabricated Bluetooth transmission board was compact at 19 mm × 12 mm. The supply voltage was designed to be 3 V such that it can be provided by a standard cell battery with a nominal voltage of 3 V. A standard I²C interface was set in connector CN3 to control the measurement board of the sensor system. The largest component on the transmission board was the Bluetooth chip (MDBT42V-512KV2, Raytac Co.), with high-performance and excellent connectivity (Fig. 3a). To realize a compact transmission module, we used the least number of components possible. Typically, a crystal oscillator, three capacitors, and three capacitor networks (CNs) were assembled on the transmission board.

D. Experimental apparatus

Sputter equipment SME-200E (Ulvac Co.) was used to deposit the material films on the wafer substrate. Mask aligner SUSS MA6/BA6 (SUSS MicroTec Co.) was used to implant the lithograph for generating the designed pattern on the photoresist. Four-point resistance processor Sigma-5 (NPS Inc.) was used to measure the sheet resistance of the fabricated sensing electrode. The topographies of the sensing material layers were measured using an atomic force

microscope (AFM) SPA-500 (SII Nanotechnology Inc.). A mixed signal oscilloscope DLM2024 (Yokogawa Electric Co.) was employed to record the flow current on the shunt resistor. A cabinet chamber LHL-114 (ESPEC Corp.) was utilized to provide a varying ambient temperature environment. Digital anatomy 3D printer J750 (Stratasys. Co.) was employed to fabricate the casing of the pH sensor module for field measurement.

III. MEASUREMENT RESULTS

A. Configuration comparison of the proposed sensor electrodes

Using the AFM, four-point resistance probe, and optical microscope, the mechanical properties of the fabricated sensing electrodes were investigated and characterized comprehensively. Table 1 shows the property comparisons of the proposed sensing electrodes. The comb- and pillar-sensing electrodes were fabricated using ITO; Ta₂O₅ and SnO₂ were examined as sensing materials for the plate-type electrode. The sizes of the proposed comb, plate, and pillar sensing electrodes were 15 mm × 4 mm, 12 mm × 9 mm, and Φ5 mm × 30 mm, respectively. Correspondingly, the contact area of these sensing electrodes were 39.0 mm², 28.3 mm², and 471 mm², respectively. As the pillar-type sensing electrode has the largest contact area under a similar electrode size, it exhibits high sensitivity, but function failure can occur due to surface contamination. Moreover, compared to the traditional two-dimensional MEMS technique, in the fabrication process of a pillar electrode, a uniform speed rotating device is required in the sputter equipment to coat the sensing film on the surface with homogeneous thickness.

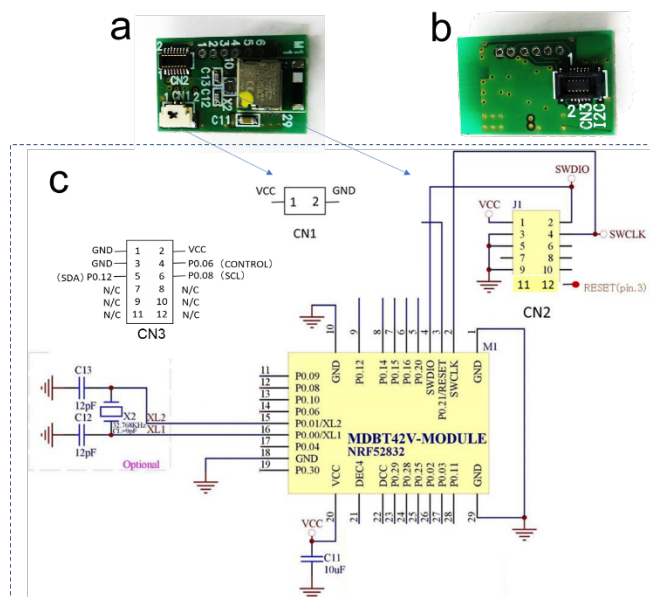


Figure 3. (a) and (b): fabricated Bluetooth transmission board; (c): circuit diagram of the Bluetooth transmission module.

TABLE I. COMPARISON OF THE SENSING ELECTRODES

Sensor type	Comb	Plate	Pillar
Electrode size	15 mm × 4 mm	12 mm × 9 mm	Φ5 mm × 30 mm
Fabrication method	Photolithography Sputtering Lift-off/Etching	Photolithography Sputtering Lift-off/Etching	Sputtering (uniform speed rolling device)
Contact area	39.0 mm ²	28.3 mm ²	471 mm ²
Sheet resistance	10 Ω/sq (Film on the SiO ₂ substrate)	SnO ₂ :0.85 Ω/sq Ta ₂ O ₅ :0.91 Ω/sq (Films on the metallic under-electrode)	10-30 Ω/sq (Films on the glass substrate)
Surface homogeneity [14]	1.1 nm (Ra)	SnO ₂ :1.2 nm (Ra) Ta ₂ O ₅ :2.5 nm (Ra)	Unmeasured

The surface roughness of the different sensing materials was measured as an arithmetical average value (Ra). For the surface topographies of the fabricated Ta₂O₅, SnO₂, and ITO, it was 2.5 nm, 1.2 nm, and 1.1 nm, respectively. The sensing films on the electrodes retained their smoothness with fewer morphological defects after the MEMS etching process. The fabricated sensing electrode had a uniform surface and was suitable for application in electronic devices. In some cases, sensing films have rough grain surfaces, which can completely obscure the material intrinsic charge transport properties [15].

B. Comparison of the electrical properties of the pH sensing materials

To characterize the electrical properties of the sensing materials and determine the performances of the fabricated sensor electrodes, we evaluated the output sensitivity of the ITO, SnO₂, and Ta₂O₅-based pH sensor electrodes. Their outputs were linear, proportional to the pH value changes, with sensitivities ranging from 0.29–0.53 mV/pH [16]. Some researchers have proposed Sb-based pH sensors for application in biosensing for better biocompatibility [17]. Therefore, in this study, we also compared the sensitivity of a typical ITO-pH sensing electrode and Sb electrode. The range of the measured pH solution was set to 4.5–7.5 because urine is weakly acidic with a pH range of 4.6–8.0 and an average of 6.0 under normal dietary conditions [18]. Fig. 4 compares the output of a typical ITO-based pH sensor electrode and an Sb-based one. The Sb sensing electrode maintains a linear output proportional to the changes in the pH value. Moreover, its output slope is similar to that of the ITO-based pH sensor; the relative error between the two sensors does not exceed 5 % on average. The minuscule difference between the slopes of the fitting curves shows that

the Sb-pH sensor electrode has a relatively high sensitivity (Fig. 4, fitting curves). Long-term stability (months of testing of deviation and drift) evaluation is in progress and will be reported in future works. After evaluating the electrical properties, we can reasonably determine the advantages and disadvantages of the sensing materials. In addition, the measured sensitivity data can be used to calibrate the proposed sensors, after which the sensor module can be used to perform field measurements to establish its stability and reliability.

C. Temperature calibration of the sensor system

The developed MEMS sensor will be used in different working conditions, and several environmental factors such as the environmental noise, humidity, and temperature may affect the sensor function. Environmental noise and humidity can be easily removed using packaging with good sealing; the temperature is critical and is generally eliminated through calibration. Therefore, temperature calibration of the proposed compact pH sensor needs to be completed before field measurements. Fig. 5 shows the voltage output of the proposed pH sensor with respect to the temperature variation. A typical ITO sensing electrode was used for demonstration. The measurement and transmission boards were placed in the cabinet chamber, and the temperature range was set from 20–60 °C. We found that the proposed pH sensor system was temperature dependent, i.e., in the measured solution with a stable pH value, the sensor voltage output increased when the environmental temperature decreased. The reason for this is that there are many electrical components, and the working resistances, in particular, are easily influenced by the environmental temperature changes. However, the output voltage deviation has a linear relationship with the temperature change; therefore, we can conclude that the calibration, i.e., output voltage, can be resolved using a first-degree polynomial equation with the temperature variation.

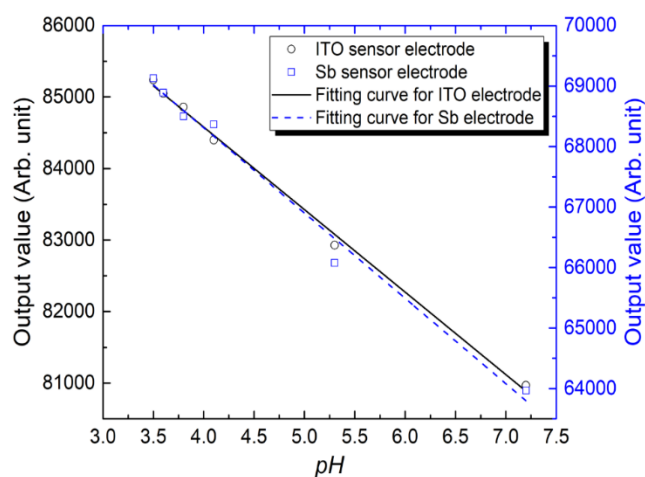


Figure 4. Comparison of output values of typical ITO- and Sb-based pH sensor electrodes.

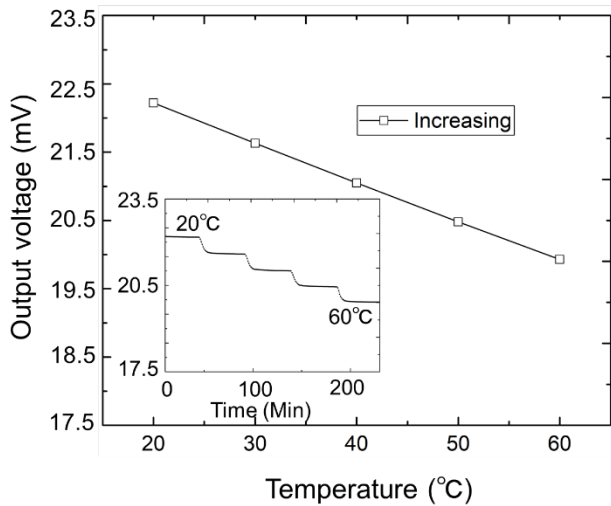


Figure 5. Temperature calibration of the proposed sensor module. Inset is the continuous record of the sensor voltage output with respect to the temperature change.

D. Power consumption of the measurement systems

The lifetime of the power supply is one of the critical issues for health monitoring sensors. Hence, we measured the power consumption of the proposed transmission approaches. To record the input current flow into the sensor’s measurement and transmission circuits, a 1-ohm shunt resistor was connected between the power supply and sensor system. An oscilloscope was used to continuously measure and record the corresponding voltage on the shunt resistor. Fig. 6 compares the input current flow of pH sensors with the RFIC transmitter and Bluetooth transmission system.

The results show that the RFIC transmitter sensor system can implement each data acquisition under a measurement average of 128 times and transmit in 250 ms. The power consumption was calculated to be 7.0×10^{-4} mAh for a one-time test. Correspondingly, the Bluetooth device had a capacity charge, stable process before the measurement operation under a 32-times data average, and the power consumption was calculated to be 2.8×10^{-4} mAh. To minimize the package size of the sensor system for user comfort, a CR1220 battery has been developed for providing the power supply in future, considering the balance between the sensor system size and battery capacity. The lifetimes of the coin cell battery for the RFIC wireless and Bluetooth sensors can be calculated and are estimated to be more than three months under a 10-min-interval measurement condition, which is a sufficient sampling rate for the real-time monitoring of the target pH value.

E. Long-term measurement of the sensor output with ambient temperature variation

The proposed compact pH sensor system has several potential applications. Typically, the sensor prototype is

placed in a diaper for monitoring the urine conditions of infants. Generally, a diaper will be used and changed within a few hours; thus, a relatively long-term measurement should be verified. Fig. 7 shows the long-term measurement results of the proposed pH sensor output and the environmental ambient temperature. The tested data were collected and recorded by a PC-based receiver for more than two days. The proposed pH sensor could continuously measure a stable solution for 48 h with a reasonable output and maintain a stable baseline. Simultaneously, a digital thermal infrared temperature sensor was loaded on the transmission board; after temperature calibration of the output voltage, the proposed sensor exhibited a highly linear output performance.

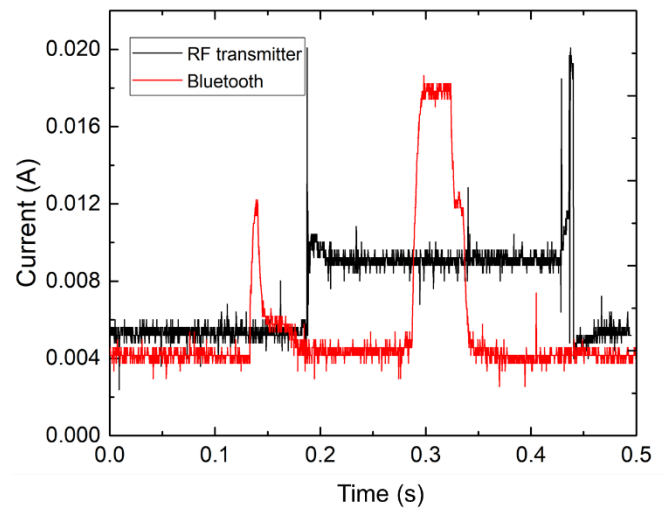


Figure 6. Input current flow comparison between pH sensors with the RFIC wireless and Bluetooth transmission systems.

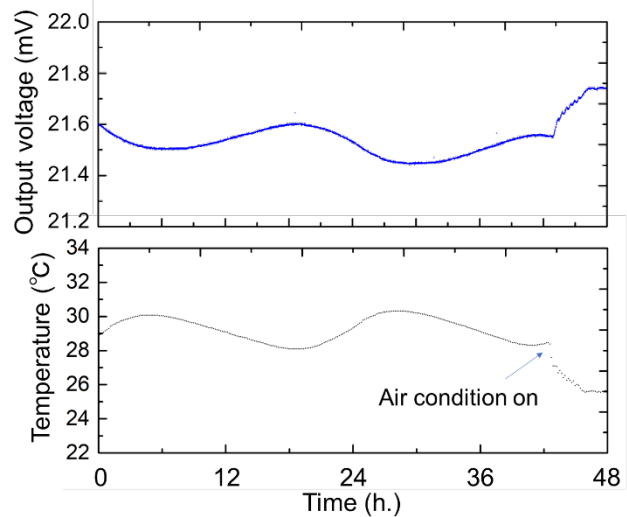


Figure 7. Long-term measurement of the proposed pH sensor voltage output at ambient environmental temperature.

IV. DEVELOPMENT OF A USER INTERFACE FOR THE PH SENSOR BASED ON AN ANDROID SMARTPHONE

A. Sensor module casing using a 3D printer for field measurement

A digital anatomy 3D printer (J750) was used for fabricating the sensor module casing using a biofriendly material. Fig. 8 depicts the casing of the pH sensor module for field measurements. The size of the sensor module case was 26 mm × 17 mm × 13 mm (inset in Fig. 8). A CR1220 (Panasonic. Co.) cell battery was placed in the battery case to provide power to the sensor system. Two signal-line wires are connected to the sensing board with the sensor electrodes. During field measurement, the sensor electrodes were placed in a layer of superabsorbent polymers, where the sensor can contact the target solution adaptably (Fig. 8). The plate and comb sensing electrodes are thin and are therefore suitable for this application. A smartphone was used to monitor the pH value via Bluetooth transmission.

B. Development of the pH sensor user interface based on an Android smartphone

Using the integrated development environment of SEGGER Embedded Studio 4.30c, a customized Android application with a friendly user interface was coded in C-language. The application program, mainly comprising the pH sensing function control and Bluetooth transmission, was successfully developed. Fig. 9 shows the user interface of the pH sensor system; a Pixel 4 smart phone (Google Co.) was used as the terminal device.

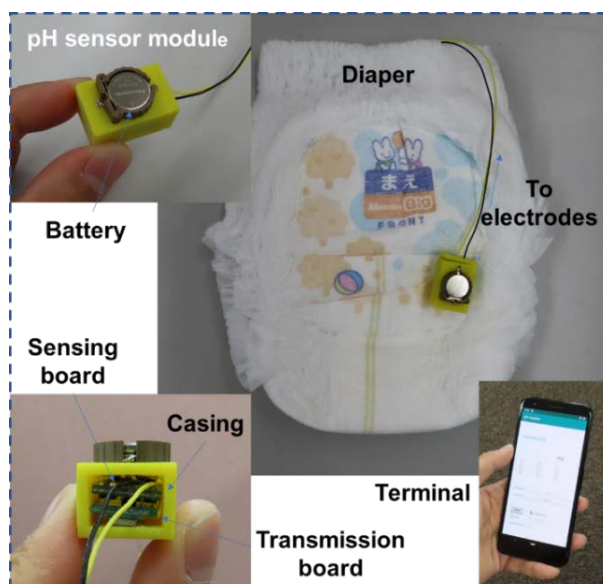


Figure 8. Casing of the pH sensor module and field measurement.

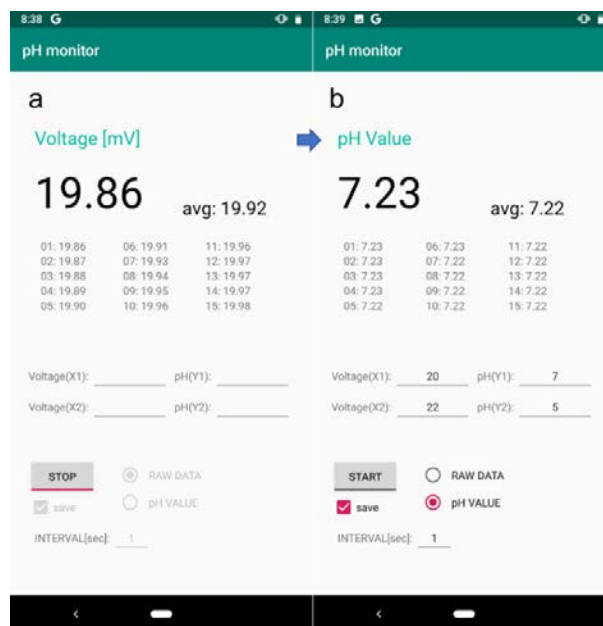


Figure 9. User interface of the wireless pH sensor system.

Fig. 9a displays the calibration page of the pH sensor system, where the primitive raw data is the voltage value of the shunt resistance. Because the calculation formula is embedded in the program, the user can calibrate the pH sensor using two different pH values with a standard reference solution or two liquids with known pH values. The conversion formula between the voltage and pH values is written in the program. Therefore, the pH sensor system can be used to measure the target solution, similar to a commercial pH sensor (Fig. 9b). In addition, the interval time can be adjusted from 1–100 s. The latest 15 data points can be directly observed on the screen, and all the data are saved in the memory with a time stamp.

V. CONCLUSION AND FUTURE WORK

In this study, a highly compact pH sensor system was developed and the extension of its application for health monitoring was discussed. Three types of sensing electrodes, plate, comb, and pillar, were fabricated and evaluated to determine the appropriate approach for different application requirements. The results indicated that the pillar type, which had the largest contact area, was suitable for complicated testing environments, whereas the comb type, which was the most compact, was suitable for use in limited space. Different sensing materials such as ITO, SnO₂, Ta₂O₅, and Sb were characterized and evaluated comprehensively. The advantages and disadvantages of these sensing materials were determined to establish their suitability for different application requirements. The SnO₂ sensing electrode exhibited the highest sensitivity for pH detection and the least output voltage, reducing the power consumption. Moreover, two types of wireless transmission boards were proposed and compared. Both had low power

consumption, suitable for long-term measurement. The proposed compact pH sensor system with adequate performance can be used in healthcare, well-being, and medical applications. Future study in this area will include further optimization of the sensor system to make it smaller and more comfortable to wear. Empirical and field experiments are also expected to be implemented as soon as possible.

ACKNOWLEDGMENT

The authors would like to thank Mr. Yoshihisa Mishima for his collaboration on the early stages of this work.

REFERENCES

- [1] L. Zhang, J. Lu, and R. Maeda, "Performance comparison of pH sensor module with wireless transmission function," The Fifth International Conference on Advances in Sensors, Actuators, Metering and Sensing (ALLSENSORS 2020), IARIA Press Mar. 2020, pp. 18-19, ISSN: 2519-836X/ ISBN: 978-1-61208-766-5.
- [2] Information on diseases & conditions for parents with infants & toddlers (Ages 0-3). [Online]. Available from: <http://www.cdc.gov/2020.07.25>
- [3] A. Symon, N. Hassan, H. Rashid, I. Ahmed, and S. Reza, "Design and development of a smart baby monitoring system based on Raspberry Pi and Pi camera," 4th International Conference on Advances in Electrical Engineering (ICAEE 2017), IEEE Press, Sept. 2017, pp. 117-122, doi: 10.1109/ICAEE.2017.8255338.
- [4] L. Manjakkal, S. Dervin, and R. Dahiya, "Flexible potentiometric pH sensors for wearable systems," RSC Adv., vol. 10, pp. 8594-8617, Feb. 2020, doi: 10.1039/D0RA00016G.
- [5] M. Obatake, T. Muraji, S. Satoh, E. Nishijima, and C. Tsugawa, "Urinary sulfated bile acids: A new simple urine test for cholestasis in infants and children," J. Pediatr. Surg., vol. 37, pp. 1707-1708, Dec. 2002, doi: 10.1053/jpsu.2002.36701.
- [6] P. Li, L. Ma, and S. Wong, "Is bag urine culture useful in monitoring urinary tract infection in infants?," J. Paediatr. Child Health, vol. 38, pp. 377-381, Aug. 2002, doi: 10.1046/J.1440-1754.2002.00010.x.
- [7] G. Ciuti, L. Ricotti, A. Menciassi, and P. Dario, "MEMS sensor technologies for human centred applications in healthcare, physical activities, safety and environmental sensing: A review on research activities in Italy," Sensors, vol. 15, pp. 6441-6468, Mar. 2015, doi: 10.3390/S150306441.
- [8] R. Bogue, "Recent developments in MEMS sensors: A review of applications, markets and technologies," Sens. Rev., vol. 33, pp. 300-304, Sept. 2013, doi: 10.1108/SR-05-2013-678.
- [9] X. Hu, Y. Wei, Y. Chen, and C. Liu, "Design of the smart pH sensor based on ion selection electrode," Sensors & Transducers, vol. 26, Special Issue, pp. 92-100, Mar. 2014, ISSN: 2306-8515, e-ISSN 1726-5479.
- [10] S. Lozovoy, A. Kukla, and A. Pavluchenko, "Investigation of metrological performance of the ISFET-based pH sensors," Sensors & Transducers, vol. 27, Special Issue, pp. 225-232, May 2014, ISSN: 2306-8515, e-ISSN 1726-5479.
- [11] L. Zhang, J. Lu, H. Okada, H. Nogami, T. Itoh, and S. Arai, "Low-power highly sensitive pH sensor with μ -dots protective structures for monitoring rumen in cows in real-time," IEEE Sens. J., vol. 17, pp. 7281-7289, Sept. 2017, doi: 10.1109/JSEN.2017.2757701.
- [12] L. Zhang, J. Lu, H. Okada, H. Nogami, and T. Itoh, "Development of ITO- and FET-based cow rumen sensor for long-term pH value monitoring," 2016 Symposium on Design, Test, Integration and Packaging of MEMS/MOEMS (DTIP 2016), IEEE Press, May 2016, pp. 92-96, doi: 10.1109/DTIP.2016.7514846.
- [13] J. Lu, L. Zhang, D. Zhang, S. Matsumoto, H. Hiroshima, R. Maeda, M. Sato, A. Toyoda, T. Gotoh, and N. Ohkohchi, "Development of implantable wireless sensor nodes for animal husbandry and medtech innovation," Sensors, vol. 18, pp. 979-1-12, Apr. 2018, doi: 10.3390/s18040979.
- [14] L. Zhang, J. Lu, R. Maeda, and H. Nogami, "Research on the performance of solid-state pH sensor affected by the sensing materials," The Fourth International Conference on Advances in Sensors, Actuators, Metering and Sensing (ALLSENSORS 2019), IARIA, Feb. 2019, pp. 1-2, ISSN: 2519-836X, ISBN: 978-1-61208-691-0.
- [15] Y. Diao, L. Shaw, Z. Bao, and S. Mannsfeld, "Morphology control strategies for solution-processed organic semiconductor thin films," Energy Environ. Sci., vol. 7, May 2014, pp. 2145-2159, doi: 10.1039/C4EE00688G.
- [16] L. Zhang, J. Lu, R. Maeda, and H. Nogami, "Research on the performance of solid-state pH sensor affected by the sensing materials," The Fourth International Conference on Advances in Sensors, Actuators, Metering and Sensing (ALLSENSORS 2019), IARIA, Feb. 2019, pp. 1-2, ISSN: 2519-836X, ISBN: 978-1-61208-691-0.
- [17] T. Kazuyoshi, A. Saad Mohammad, K. Daiki, K. Kagemasa, and K. Minoru, "Development of one electrode type pH sensor measuring in microscopic Region," Int. J. Appl. Electron., vol. 52, pp. 1417-1424, Dec. 2016, doi: 10.3233/JAE-162139.
- [18] What is the normal pH range of urine? Available from: <http://www.medicalnewstoday.com/2020.12.09>